Supporting Information

Pedersen et al. 10.1073/pnas.0901202106

SI Text

Equations. Granule compartments measured in number of granules. Abbreviations as in Fig. 1 except AP, "almost-docked pool;" FIP, F_{IRP}; RIP, R_{IRP}; FHP, F_{HCSP}; and RHP, R_{HCSP}.

$$IRP' = r_1\,PP - r_{-1}\,IRP - f_I(C_{md})IRP, \quad [1]$$

$$PP' = r_{-1}\,IRP - (r_1 + r_{-2})PP + r_2\,DP, \quad [2]$$

$$DP' = r_3\,HCSP + r_{-2}\,PP - (r_{-3} + r_2)DP, \quad [3]$$

$$HCSP' = r_4\,AP - (r_{-4} + r_3)HCSP + r_{-3}\,DP - f_H(C_i)HCSP, \quad [4]$$

$$AP' = r_5 - (r_{-5} + r_4)\,AP + r_{-4}\,HCSP, \quad [5]$$

$$FIP' = f_I(C_{md})IRP - u_2\,FIP, \quad [6]$$

$$RIP' = u_2\,FIP - u_3\,RIP, \quad [7]$$

$$FHP' = f_H(C_i)HCSP - u_2\,FHP, \quad [8]$$

$$RHP' = u_2 FHP - u_3 RHP. \quad [9]$$

Fusion rates from IRP (f_I) and HCSP (f_H) follow Hill functions.

$$f_I(C_{md}) = f_{I,\max}\frac{C_{md}^n}{C_{md}^n + K_I^n}, \quad f_H(C_i) = f_{H,\max}\frac{C_i^n}{C_i^n + K_H^n}, \quad [10]$$

where C_{md} is the Ca^{2+} concentration in microdomains, C_i the bulk cytosolic Ca^{2+} concentration, measured in micromolar.

Calcium compartments are modeled as in Chen et al. (9) and described by

$$C'_{md} = -f_{md}J_L - f_{md}B(C_{md} - C_i), \quad [11]$$

$$C'_i = -f_i\,J_R + f_v f_i B(C_m d - C_i) - f_i\,L. \quad [12]$$

Molar fluxes through L- and R-type channels:

$$J_L = \alpha I_L/v_{md}, \qquad J_R = \alpha I_R/v_{cell}. \quad [13]$$

where the respective currents are

$$I_L = g_L m_\infty(V)(V - V_{Ca}), \qquad I_R = g_R m_\infty(V)(V - V_{Ca}), \quad [14]$$

with $m_\infty(v) = 1/(1 + \exp((V_m - V)/s_m))$.

Calcium pumps and stores

$$J_{serca} = J_{serca,\max}\frac{C_i^2}{K_{serca}^2 + C_i^2}, \; J_{pmca} = J_{pmca,\max}\frac{C_i}{K_{pmca} + C_i}, \quad [15]$$

$$J_{ncx} = J_{ncx,0}(C_i - 0.25\mu M),\; L = J_{serca} + J_{pmca} + J_{ncx} + J_{leak}. \quad [16]$$

To follow capacitance increases, the fusion fluxes are multiplied by 3.5 fF per granule and integrated, i.e.,

$$Cap_{IRP} = 3.5\int_0^t f_I\,IRP, \quad Cap_{HCSP} = 3.5\int_0^t f_H\,HCSP. \quad [17]$$

Similarly, to follow secretion, the release fluxes are multiplied by 9 pg per granule per islet (see ref. 1) and by 60 to change from seconds to minutes.

$$Secr_{IRP} = 60 \cdot 9 \cdot u_3 RI, \quad Secr_{HCSP} = 60 \cdot 9 \cdot u_3 RH. \quad [18]$$

We show mainly the 2-min moving averages of these expression.

Initial Conditions. All simulations are started from steady-state. For the standard parameters (see below) this yields the following initial conditions: IRP(0) = 7.69, PP(0) = 38.45, DP(0) = 297.17, HCSP(0) = 12.06, AP(0) = 964.8, FIP(0) = 1.5×10^{-7}, RIP(0) = 2.3×10^{-5}, FHP(0) = 8×10^{-5}, RHP(0) = 0.012, $C_{md}(0)$ = 0.0674 μM, $C_i(0)$ = 0.06274 μM.

Parameters. Vesicle dynamics parameters (s^{-1}): $r_1 = 0.005$, $r_{-1} = 0.025$, $r_2 = 0.00014$, $r_{-2} = 0.001$, $r_3 = 0.00185$, $r_{-3} = 0.00007$, $r_4 = 0.002$, $r_{-4} = 0.16$, $r_5 = 0.22$, $r_{-5} = 0.0002$, $u_1 = 2000$, $u_2 = 3$, $u_3 = 0.02$.

Fusion constants: $f_{I,\max} = 30\ s^{-1}$, $K_I = 22\ \mu M$, $f_{H,\max} = 30\ s^{-1}$, $K_H = 2.5\ \mu M$, $n = 4$.

Calcium currents: $g_L = 150$ pS, $g_R = 150$ pS, $V_m = -20$ mV, $V_{Ca} = 25$ mV, $s_m = 5$ mV.

Calcium fluxes: $J_{serca,max} = 41\ \mu M/s$, $K_{serca} = 0.27\ \mu M$, $J_{pmca,max} = 2{,}141\ \mu M/s$, $K_{pmca} = 0.5\ \mu M$, $J_{leak} = -0.9441\ \mu M/s$, $J_{ncx,0} = 18.67\ s^{-1}$, $f_{md} = 0.01$, $f_i = 0.01$, $B = 17{,}250\ s^{-1}$, $\alpha = 5.18\ 10^{-15}\ \mu mol/s/fA$, $v_{cell} = 1.15$ pl, $v_{md} = 0.00385\ 10^{-3}$ pl, $f_v = v_{md}/v_{cell}$.

1. Chen Y, Wang S, Sherman A (2008) Identifying the targets of the amplifying pathway for insulin secretion in pancreatic beta-cells by kinetic modeling of granule exocytosis. *Biophys J* 95:2226–2241.

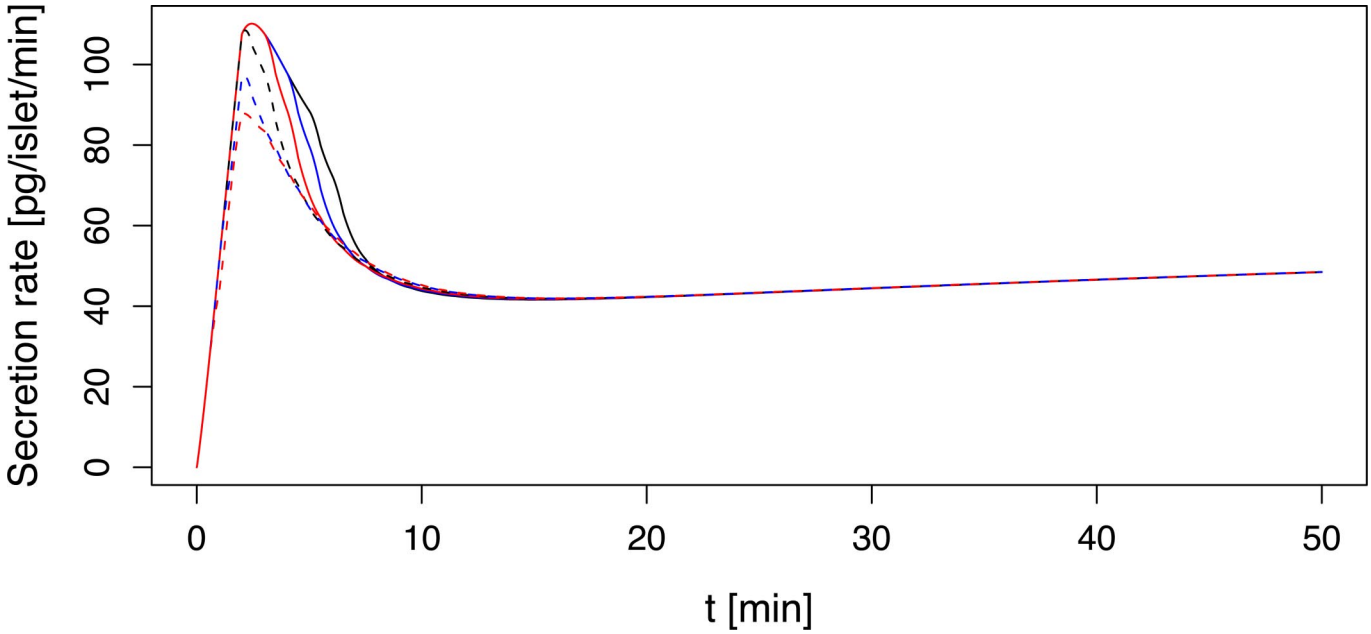

Fig. S1. Two-minute moving average of total secretion rates due to an imposed burst-like pattern with a period of 1 min. The length of the depolarization was varied from 30 s (dashed red), through 1 min (dashed blue), 2 min (dashed black), 3 min (solid red), 4 min (solid blue) to 5 min (solid black). (see ref. 1).

1. Henquin J-C, Nenquin M, Stiernet P, Ahren B (2006) In vivo and in vitro glucose-induced biphasic insulin secretion in the mouse: Pattern and role of cytoplasmic Ca^{2+} and amplification signals in beta-cells. *Diabetes* 55:441–451.

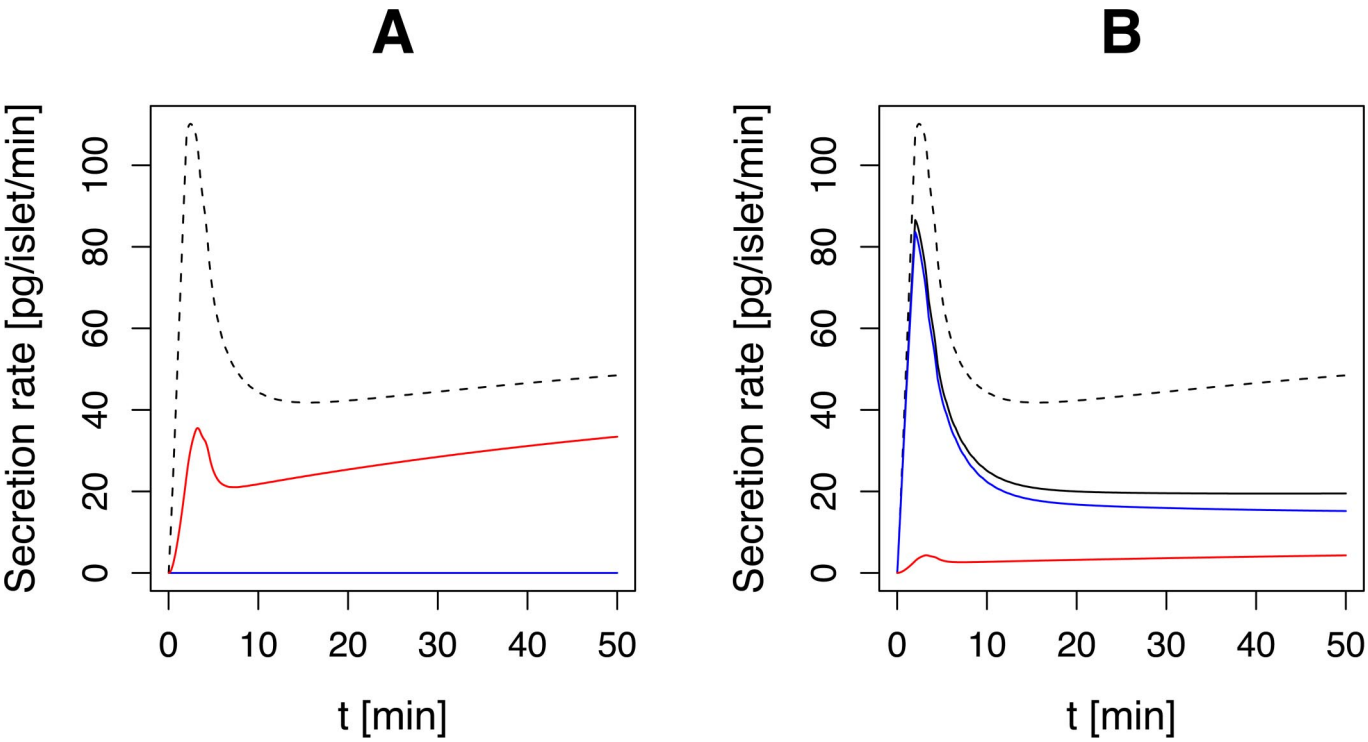

Fig. S2. Two-minute moving average of total secretion rates with an imposed burst-like pattern with a period of 1 min. (*A*) L-type knockout [g_L set to zero, and g_R = 300 pS up-regulated to compensate (1)]. (*B*) R-type knock-out (2) (g_R = 0 pS). Legends as in Fig. 3. For comparison, the dashed line taken from Fig. 3 shows total wild-type release.

1. Schulla V, et al. (2003) Impaired insulin secretion and glucose tolerance in beta cell-selective Ca(v)1.2 Ca^{2+} channel null mice. *EMBO J* 22:3844–3854.
2. Jing X, et al. (2005) CaV2.3 calcium channels control second-phase insulin release. *J Clin Invest* 115:146–154.

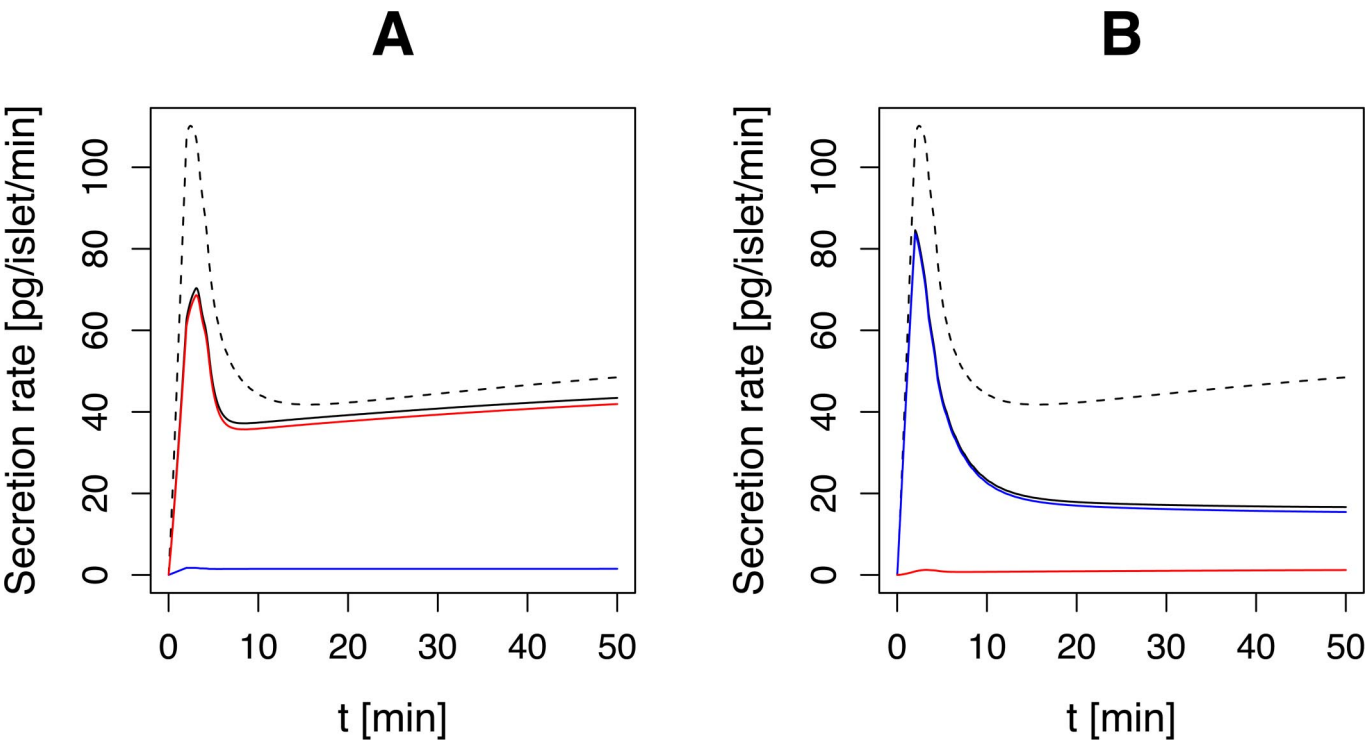

Fig. S3. Two-minute moving average of total secretion rates with an imposed burst-like pattern with a period of 1 min. (*A*) Synt1A knockout (low docking rate, r_3 reduced 90%) (1). (*B*) Hypothetical knockout of HCSP Ca^{2+} sensor (fusion from the HCSP lowered by a factor of 30). Legends as in Fig. 3. For comparison, the dashed line taken from Fig. 3 shows total wild-type release.

1. Ohara-Imaizumi M, et al. (2007) Imaging analysis reveals mechanistic differences between first- and second-phase insulin exocytosis. *J Cell Biol* 177:695–705.

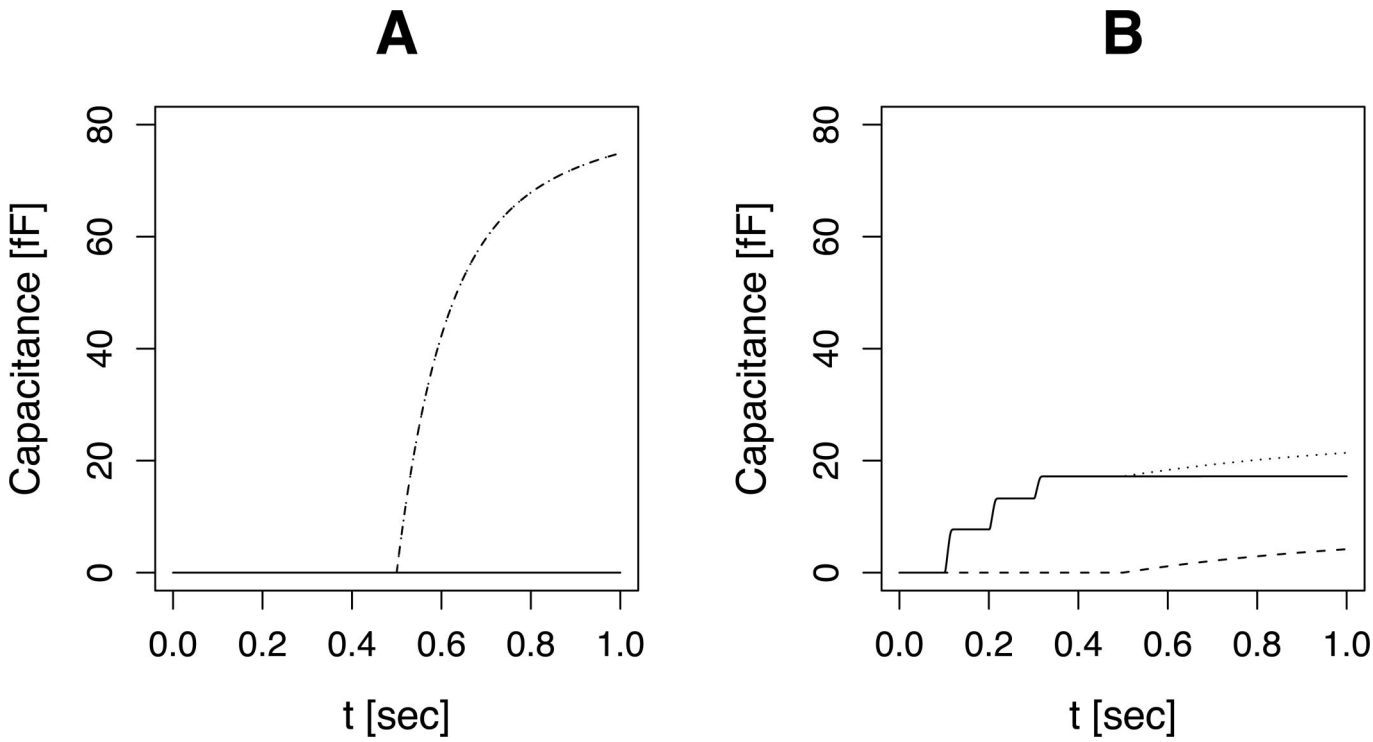

Fig. S4. (*A*) Predicted fast HCSP protocol for Synt-1A knockout (1). Parameters are as in Fig. S3*A*. (*B*) Predicted fast HCSP protocol for hypothetical knockout of HCSP Ca^{2+} sensor. Parameters are as in Fig. S3*B*.

1. Ohara-Imaizumi M, et al. (2007) Imaging analysis reveals mechanistic differences between first- and second-phase insulin exocytosis. *J Cell Biol* 177:695–705.